ACCSCIENCE PUBLISHING

International Journal of Bioprinting

RESEARCH ARTICLE

# Inkjet bioprinting of NE-4C neural progenitor cells with enhanced neuronal differentiation via retinoic acid treatment

**Xinda Li[1,2†], Xiaolei Guo[3,4†], Jinzhou Feng[1], Lihua Chen[1], Huan Xiong[1], Ruxiang Xu[1*], and Tao Xu[1,2,5*]**

[1]Department of Neurosurgery, Sichuan Provincial People's Hospital, University of Electronic Science and Technology of China, Chengdu, Sichuan, China

[2]Department of Mechanical Engineering, School of Mechanical Engineering, Tsinghua University, Beijing, China

[3]Center for Medical Device Evaluation, National Medical Products Administration, Beijing, China

[4]State Key Laboratory of Tribology, Department of Mechanical Engineering, School of Mechanical Engineering, Tsinghua University, Beijing, China

[5]Center for Bio-intelligent Manufacturing and Living Matter Bioprinting, Research Institute of Tsinghua University in Shenzhen, Tsinghua University, Shenzhen, Guangdong, China

## Abstract

During inkjet bioprinting, cells are subjected to direct shear stress as they pass through the nozzles, causing reversible deformation of the cell membranes and potentially triggering subcellular changes, such as activation of molecular pathways, leading to beneficial outcomes. In this study, neural progenitor NE-4C cells were printed through 30μm thermal inkjet nozzles. Compared to manually pipetted cells (control group), bioprinted cells (inkjet group) exhibited several distinct changes, such as reduced cell proliferation during the first four days after bioprinting, increased tolerance to high-concentration retinoic acid, and significantly elevated expression of the early neuronal marker class III β-tubulin, indicating enhanced neuronal differentiation. Furthermore, RNA sequencing and enrichment analysis further revealed upregulation of cell metabolism pathways in the bioprinted group. Collectively, these findings suggest that inkjet bioprinting may be a promising strategy to accelerate neural tissue formation, warranting further studies.

***Keywords:*** Inkjet bioprinting; Neural differentiation; Neural progenitor cells

## 1. Introduction

Inkjet bioprinting possesses exceptional capability to deliver biological components and form high-resolution patterns in a sterile, economical, and high-throughput manner.[1,2] To date, inkjet bioprinting has evolved as a powerful tool for tissue engineering and regenerative medicine, enabling the fabrication of biomaterial scaffolds,[3-5] biomolecule gradients[6-8] and cell patterns.[9-15] Consequently, inkjet bioprinting has been regarded as one of the mainstream bioprinting strategies.[16,17] Moreover, it is feasible to print living cells with minimal damage using this approach.[18-20] Generally, inkjet bioprinting

†These authors contributed equally to this work.

***Corresponding authors:**
Tao Xu
(xut@tsinghua-sz.org)

Ruxiang Xu
(xuruxiang1123@uestc.edu.cn)

**Citation:** Li X, Guo X, Feng J, *et al*. Inkjet bioprinting of NE-4C neural progenitor cells with enhanced neuronal differentiation via retinoic acid treatment. *Int J Bioprint.* 2025;11(5):217-230. doi: 10.36922/IJB025260245

**Received:** June 24, 2025
**Revised:** July 22, 2025
**Accepted:** July 25, 2025
**Published Online:** July 25, 2025

operates via a drop-on-demand (DOD) mechanism, generating droplets containing only one or a few cells.[21-22] Due to this inherent feature, inkjet bioprinting confers practical value in cell isolation, single-cell analysis, and cell cryopreservation.[23-26]

During inkjet bioprinting, cells pass through narrow, cell-sized orifices and are therefore subjected to velocity-induced shear stress, which can cause temporary disruption of the cell membrane. Leveraging this phenomenon, Xu *et al.*[27] successfully transfected pmax green fluorescent protein plasmids into living porcine aortic endothelial cells by bioprinting a cell plasmid suspension with a thermal inkjet printer.[27] Cui *et al.*[28] further demonstrated the existence of ≈105Å transient pores on cell membranes during thermal inkjet bioprinting.[28] Sohrabi *et al.*[29] performed numerical simulation and found that the areal strain could generate multiple pores on the cell membrane during inkjet bioprinting without compromising overall cell viability.[29] This conclusion is consistent with experimental results, supporting the notion that membrane disruption caused by inkjet bioprinting may be beneficial.

Inkjet printing could facilitate neural tissue formation by depositing macromolecule patterns or fabricating electrode arrays to regulate stem cell fate.[7,30,31] Moreover, neural cells could be directly deposited to form neural tissue with inkjet bioprinting.[32,33] For instance, Tse *et al.*[32] printed neuronal analog NG108-15 cells with a piezoelectric inkjet system and found that the inkjet-printed neuronal cells expressed longer neurites at earlier stages compared to manually pipetted cells. This phenomenon may result from the piezoelectric effect, shear stress, or a combination of both applied directly to the cells.[32] These results indicate that the close contact between cells and nozzles could directly affect cellular behavior. Solis *et al.*[34] printed human microvascular endothelial cells with a thermal inkjet system. Compared with manually pipetted cells, printed endothelial cells showed elongated morphology and significant overexpression of several angiogenesis cytokines.[34] However, how inkjet bioprinting influences cellular behavior remains unclear, and further experimental evidence is needed.[35] Therefore, exploring neural cell behavior during inkjet bioprinting remains of great significance.

NE-4C is a p53-deficient immortalized neuroectodermal progenitor cell line derived from cerebral vesicles of E9-12 mouse embryos. It has been reported that NE-4C cells maintain stable karyotypes and exhibit neural differentiation both *in vitro* and *in vivo*.[36,37] The neural differentiation of NE-4C could also be triggered by all-trans retinoic acid (RA) at appropriate concentrations.[37,38] In this study, NE-4C cells were printed using a thermal inkjet printer (Figure 1). Since RA

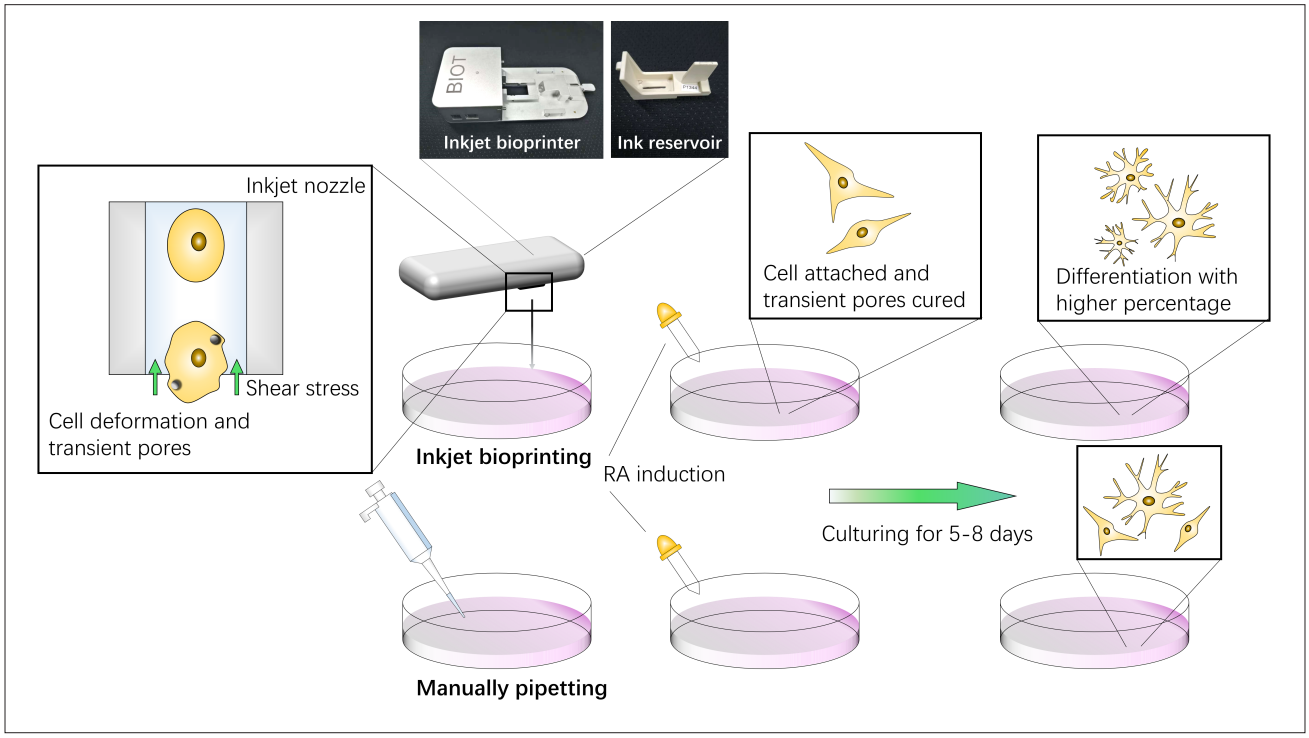


**Figure 1.** Schematic view of the experimental design. Abbreviation: RA: Retinoic acid.

receptors (RARs) and retinoid X receptors (RXRs) are located in the nucleus,[39,40] we hypothesized that thermal inkjet printing could facilitate RA transfer by creating transient pores on cell membranes. We first demonstrated the formation of transient pores on NE-4C cell membranes via calcein-acetoxymethyl (AM)/propidium iodide (PI) staining. RA treatment was applied immediately after inkjet printing for 48 hours. Nestin and class III β-tubulin (TuJ1) immunostaining were performed on days 5 and 8 post-RA treatment to detect the differentiation profiles of inkjet-bioprinted versus manually pipetted NE-4C cells. Furthermore, the cell counting kit-8 (CCK-8) assay showed that inkjet-printed NE-4C cells exhibited higher viability at high RA concentrations ($10^{-5}$ to $10^{-4}$M). Finally, RNA sequencing (RNA-seq) was performed at day 3 post-printing to evaluate differences in gene expression between inkjet-printed and manually pipetted NE-4C cells.

## 2. Materials and methods

### 2.1. Cell culture

NE-4C cell line (ATCC, CRL-2925™) was provided by the Stem Cell Bank, Chinese Academy of Sciences. The cells were cultured in minimum essential medium (MEM; 11090081, Gibco, United States) supplemented with 10% fetal bovine serum (10099141, Gibco, United States), 1% GlutaMAX™ (35050, Gibco, United States), and 1% non-essential acids (11140, Gibco, United States) at 37° in 5% carbon dioxide.

### 2.2. Inkjet bioprinting

The equipment used in this experiment was a self-developed thermal inkjet cell printer (BioT Athena) kindly provided by Shanghai Industrial μTechnology Research Institute (Figure 1). Before printing, NE-4C cells were digested and resuspended in 3% sodium chloride solution, serving as the bioink. Then, 100μL of bioink was loaded into the ink reservoir of the printhead. The printing voltage was maintained at a constant 10.8 V. During printing, each of the 325 printing nozzles was set to fire between 1,000 to 5,000 times. A 6-cm culture dish containing 1 to 2 mL MEM was placed below the printhead to collect the ejected droplets as biopaper.

### 2.3. Membrane integrity evaluation

Calcein-AM/PI staining was performed to evaluate the membrane integrity after inkjet bioprinting. As previously reported, PI could penetrate living-cell membranes exhibiting transient pores larger than approximately 16 Å.[28] Briefly, cells were cultured in MEM for at least an hour to ensure full attachment to the Petri dishes. The culture medium was then removed, and 1–2 mL of staining solution containing 2 μM calcein-AM and 8 μM PI was added. After incubation for 10 minutes, the Petri dishes were washed with phosphate buffer saline. Cells stained red or green were counted under a fluorescence microscope (Nikon Eclipse Ti2-u, Japan).

### 2.4. Cell proliferation evaluation

Alamar Blue assay was performed to depict NE-4C proliferation profile after inkjet bioprinting. Briefly, NE-4C cells were bioprinted into a 6-well plate with $1 \times 10^4$ cells in each well. Meanwhile, an equal density of cells was manually pipetted into the wells as the control group. On days 1, 4, 7, and 10 after bioprinting, 3 mL of Alamar Blue (Yeasen Biotechnology, China) working solution (1 Alamar Blue: 9 MEM) was added to each well and incubated for three hours. Optical density (OD) values were obtained on the microplate reader at wavelengths of 570 and 600 nm. For data presentation, all OD values were normalized to those on day 1.

### 2.5. NE-4C differentiation and cell counting kit-8 assay

As previously reported, NE-4C is an RA-inducible cell line that is insensitive to conventional neural differentiation factors such as basic fibroblast growth factor and epidermal growth factor.[37] Generally, a 48-hour RA treatment is sufficient to induce NE-4C differentiation into neurons or astrocytes.[36,37] Therefore, RA treatment was applied here to explore whether inkjet bioprinting affects NE-4C differentiation. All-trans RA (R2625, Sigma-Aldrich, United States) was dissolved in dimethyl sulfoxide at $10^{-1}$ mol/L as a stock solution and stored at−20° before use. Thermal-inkjet-printed NE-4C cells were set as the experimental group, and manually pipetted cells served as the control group.

For the CCK-8 cytotoxic assay, cells from each group were seeded in a 96-well plate at a density of $2\times10^3$ cells in each well. During induction, NE-4C cells were incubated in supplemented MEM with RA at concentrations of 0, $10^{-6}$, $10^{-5}$, and $10^{-4}$ mol/L for 48 hours. No extra growth factors were added throughout the process. After induction, the culture medium was carefully removed, and the CCK-8 assay was performed following the manufacturer's instructions. Briefly, 100 μL of CCK-8 (CK04, Dojindo Laboratories, Japan) working solution was added to each well and incubated for two hours. OD values were obtained on a microplate reader at a wavelength of 450 nm.

### 2.6. Immunofluorescence staining

According to the literature, NE-4C cells exhibit neuronal characteristics 3–4 days after RA induction.[36,37] Immunostaining with neural stem cell marker Nestin and early neuron marker TuJ1 was performed on days 5 and 8 post-RA treatment. Briefly, NE-4C cells in the experimental

and control groups were seeded in a 24-well plate and underwent RA treatment for 48 hours as described in **Section 2.4**. Subsequently, the cells were maintained in supplemented MEM without additional treatment. At each time point for immunostaining, the culture medium was removed, and 3 mL of 2.5% glutaraldehyde was added to each well for 30 minutes. Following fixation, blocking solution (Keygen Biotech, China) was added for another 30 minutes. Anti-Nestin (ab11306, Abcam, United Kingdom) and anti-βIII tubulin (ab18207, Abcam, United Kingdom) primary antibodies were diluted in the manufacturer-supplied diluent to the recommended concentrations. Then, 500 μL of the primary antibody solutions were added to each well and incubated overnight at 4˚C. On the following day, samples were incubated in secondary antibody solution (diluted in secondary antibody diluent) for an hour. Finally, 4',6-diamidino-2-phenylindole solution was added for 10 minutes, and fluorescent images were taken under a fluorescence microscope. Moreover, anti-Notch1 (ab52627, Abcam, United Kingdom) immunostaining was performed on NE-4C cells without RA treatment at day 4 after inkjet bioprinting, following the same procedure described above.

### 2.7. RNA sequencing

As previously reported, thermal inkjet bioprinting can influence cellular gene expression through heat shock or other relevant mechanical factors.[34] Therefore, RNA sequencing was performed to compare the transcriptomic profiles of the inkjet-printed cells and the control group. Briefly, at day 3 after bioprinting, NE-4C cells from the inkjet group and the control group were harvested and stored at 80°. The samples were then sent for sequencing and analysis. The RNA sequencing and sequencing data analysis were performed by Novogene Co., Ltd. (China).

### 2.8. Statistical analysis

Two-way analysis of variance was used to compare means across multiple groups with three replicates for each. Paired Student's *t*-test was used to compare means across single groups with five replicates. Statistical significance was determined at $^{*}p < 0.05$, $^{**}p < 0.01$, and $^{***}p < 0.001$. Data analysis was performed using GraphPad Prism 5 software.

## 3. Results

### 3.1. Number of cell-containing droplets

In the pre-experiment, bioinks with cell concentrations of 2 ×1 $0^6$/mL, 5 × $10^6$/mL, and 1 ×$10^7$/mL were printed on empty culture dishes. The number of cell-containing droplets was recorded under a microscope. The number of cell-containing droplets for these three different concentrations is listed in Table 1. The results are consistent with a previous study, reporting that the cell-containing droplet percentage increased with cell concentration.[21] However, among the cell-containing droplets, the proportion of droplets containing a single cell may decrease as cell concentration continues to increase, due to a higher frequency of droplets containing more than one cell. Therefore, the bioink with a cell concentration of 5 × $10^6$/mL was selected for further experiments for a higher frequency of single-cell-containing droplets.

### 3.2. Permeability variation of NE-4C membranes during inkjet printing

As previously reported, transient pores may form during thermal inkjet bioprinting due to the combined effects of thermal heat and mechanical stress. PI could penetrate cells through the transient pores (>16Å) on cell membranes.[28] In this experiment, calcein-AM/PI staining was performed at one hour and one day after bioprinting. Manually pipetted NE-4C cells served as the control group. NE-4C cells with green or red fluorescence were counted under a fluorescence microscope. An hour after printing, a portion of the cells in view were stained green while others were stained red (Figure 2). A total of 61 cells were observed, of which 35 were stained green while 25 cells were stained red, indicating that around 42.62% of the cells exhibited transient pores one hour after bioprinting. One day after bioprinting, all attached cells in view were stained green, as dead cells had detached (Figure 2B). In contrast, all manually pipetted cells were stained green at one hour after bioprinting (Figure 2C).

**Table 1. Number of cell-containing droplets under different cell concentrations**

| Cell concentration (/mL) | Total number of droplets (N) | Number of cell-containing droplets ($N_1$) | Number of single-cell-containing droplets ($N_2$) | Percentage of cell-containing droplets ($N_1$/N) | Percentage of single-cell-containing droplets ($N_2$/$N_1$) |
|---|---|---|---|---|---|
| 2×$10^6$ | 162 | 12 | 11 | 7.41% | 91.67% |
| 5×$10^6$ | 135 | 35 | 27 | 25.93% | 77.14% |
| 1×$10^7$ | 136 | 40 | 26 | 29.41% | 65% |

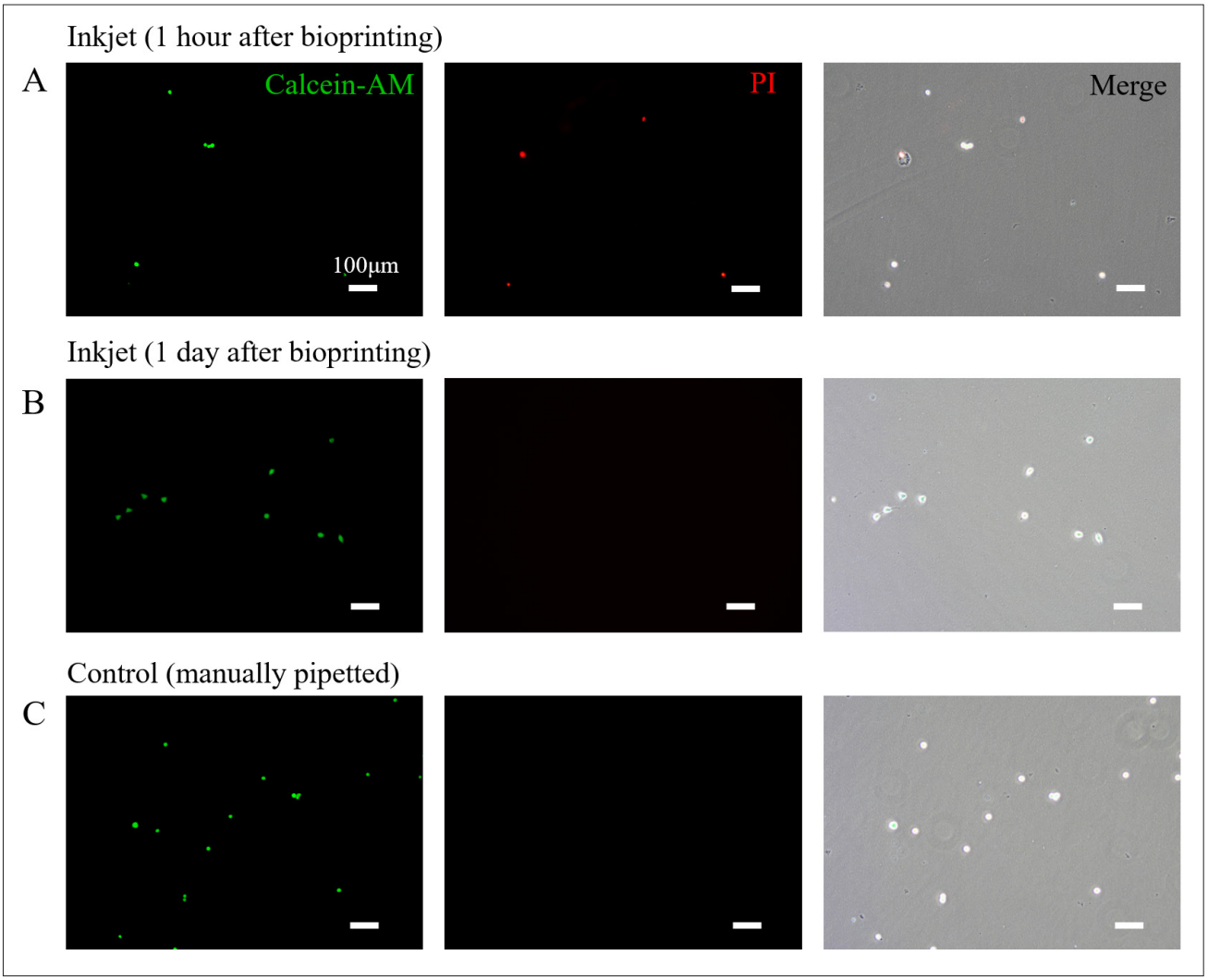


**Figure 2.** Calcein-acetoxymethyl (AM)/propidium iodide (PI) staining of NE-4C cells after inkjet printing. (A) Fluorescent images of NE-4C cells one hour after bioprinting, and (B) one day after printing. (C) Manually pipetted NE-4C cells. Scale bar: 100 μm, magnification: 100×.

### 3.3. NE-4C proliferation profile after inkjet printing

Inkjet-bioprinted and manually pipetted NE-4C cells were cultured at the same initial density for microscopic evaluation. A difference in the proliferation rate emerged at day 4 after bioprinting, with NE-4C cells in the control group showing a larger increment. By day 7, prominent cell propagation was observed in the inkjet group, while cells in the control group had nearly reached confluence. NE-4C cells in the inkjet group reached confluence at day 10, and clusters formed on the surface of the cell layer in the control group (Figure 3A & B). Results of the Alamar Blue assay are shown in Figure 3C and D. As depicted, the general tendency is similar to that observed under a microscope. Cells in the inkjet group showed minimal proliferation during the initial four days, followed by persistent multiplication until day 10. On the contrary, cells in the control group proliferated rapidly during the initial four days and gradually reached confluence, which dampened their multiplication from day 4 to day 10 (Figure 3C & D).

### 3.4. Differentiated induction of inkjet-printed NE-4C with retinoic acid

#### *3.4.1. Cytotoxicity measurement post-retinoic acid treatment*

All-trans RA with three different concentrations was used to treat inkjet-bioprinted or manually pipetted NE-4C cells for neural differentiation. CCK-8 assay was performed to measure the cytotoxicity after 48 hours of RA treatment. Briefly, at RA concentration of $10^{-6}$M, the inkjet group sustained a relative viability of 0.88±0.02 while the control

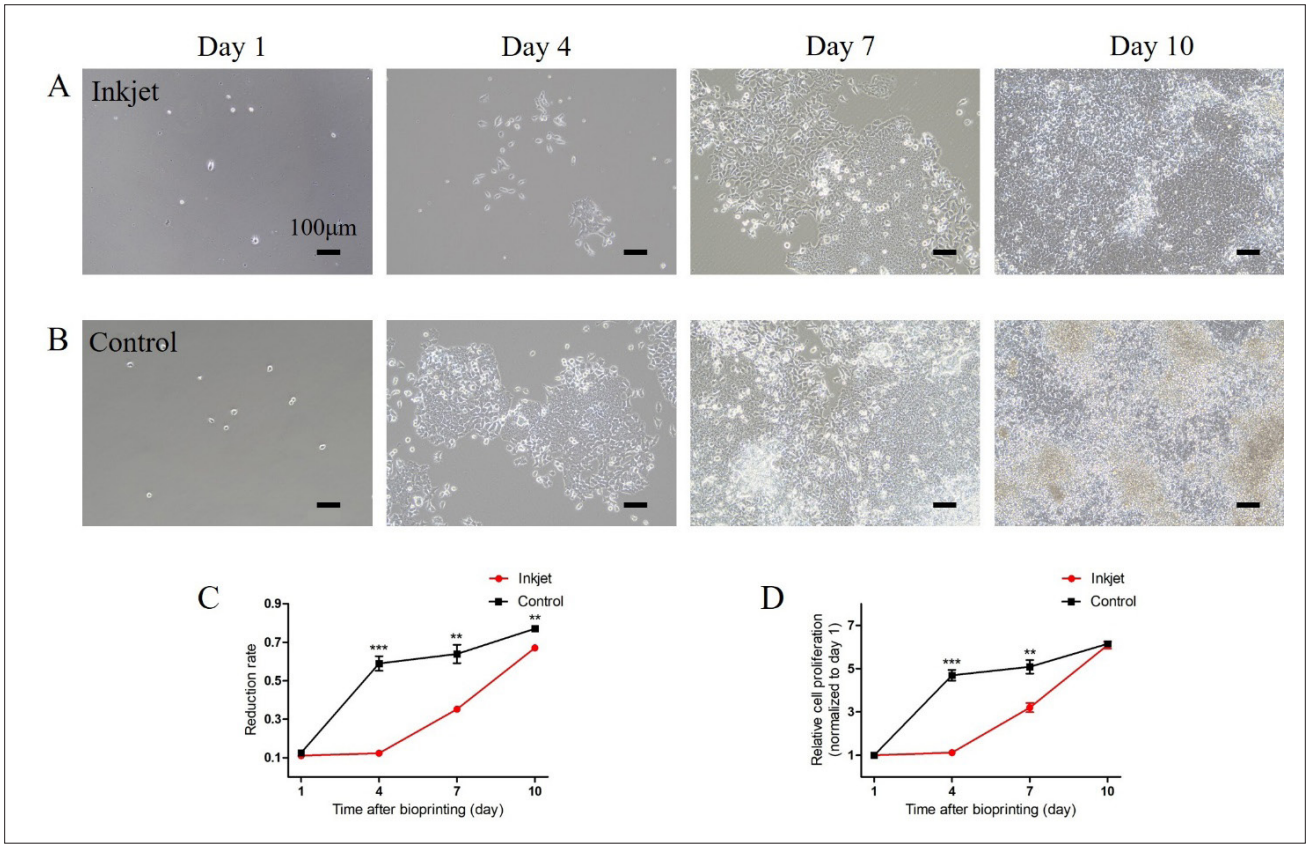


**Figure 3.** Microscopy images and proliferation profiles of inkjet-printed (inkjet) and manually pipetted (control) NE-4C cells from day 1 to day 10 post-printing. (A) Microscopy images of inkjet-printed NE-4C cells from day 1 to day 10. Scale bar: 100 μm, magnification: 100×. (B) Microscopy images of manually pipetted NE-4C cells. Scale bar: 100 μm, magnification: 100×. (C) The reduction rate of Alamar Blue stain on each corresponding day. (D) Relative proliferation rate by normalizing all values to day 1. Statistical significance determined at $^{**}p<0.01$, $^{***}p<0.001$.

group only achieved a relative viability of 0.46±0.12. At an RA concentration of $10^{-5}$M, the relative viability of the inkjet group and the control group was 0.84±0.14 and 0.44±0.17, respectively. Furthermore, for both groups, complete cell death occurred at an RA concentration of $10^{-4}$M (Figure 4). These results indicate that inkjet-bioprinted NE-4C cells presented higher viability at RA concentrations ranging from $10^{-6}$M to $10^{-5}$M.

### *3.4.2. NE-4C differentiation post-retinoic acid treatment*

NE-4C cells are derived from cerebral vesicles. As reported, Notch1 is a key regulator for neural stem cell maintenance, and inhibition of Notch1 signaling could lead to eventual depletion of hippocampal neural stem cells.[41] Therefore, prior to RA treatment, Notch1 immunostaining was performed at day 4 post-bioprinting to evaluate the stemness of NE-4C following inkjet bioprinting. The results are shown in Figure 5. NE-4C cells in both groups were Notch1-positive, with similar fluorescence intensity, indicating that the differentiation capability of NE-4C cells was not affected by inkjet bioprinting.

After 48 hours of RA treatment at a concentration of $10^{-6}$M, immunofluorescence staining of neural progenitor cell marker Nestin and neuron marker TuJ1 was performed on Day 5. The results are presented in Figure 6. In both groups, most NE-4C cells were Nestin-positive and showed morphological changes, including neurite sprouting, which distinguished them from undifferentiated NE-4C cells (Figure 6A & B). A portion of cells in both groups were TuJ1-positive, indicating the initiation of neural differentiation (Figure 6A & B). The average fluorescence intensities of Nestin and TuJ1 were measured with Image J (version ImageJ 1.53t). For Nestin, the average fluorescence intensities for the inkjet and control groups were 58.17±6.32 and 50.23±10.60, respectively ($n$=5). For TuJ1, the average fluorescence intensities for the inkjet and control groups were 86.09±13.98 and 75.93±7.15, respectively ($n$=5). No statistical significance was observed between these two groups for both markers (Figure 6C & D).

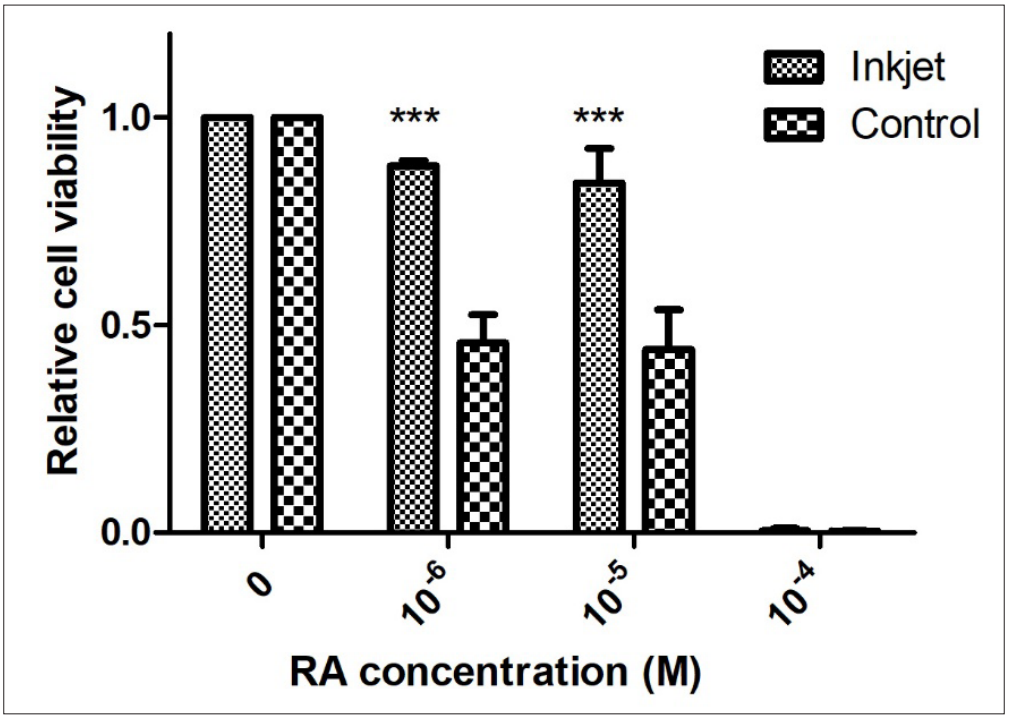


**Figure 4.** Retinoic acid (RA) susceptibility of inkjet-printed (inkjet) and manually pipetted (control) NE-4C cells. Statistical significance determined at ***$p$<0.001.

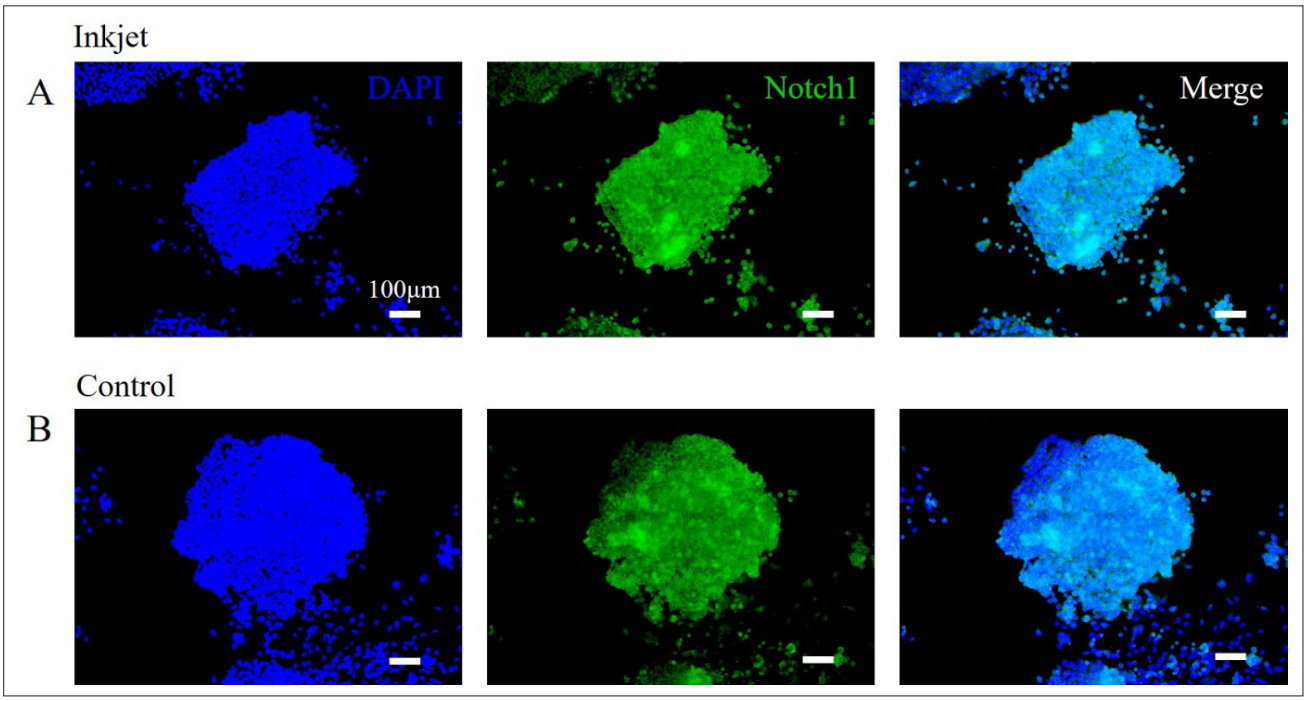


**Figure 5.** Notch1 immunofluorescence staining of inkjet-printed (inkjet) and manually pipetted (control) NE-4C cells at day four after printing. (A) Fluorescent images of Notch1 for the inkjet group. (B) Fluorescent images of Notch1 for the control group. Scale bar: 100 μm, magnification: 100×. Abbreviation: DAPI: 4',6-diamidino-2-phenylindole.

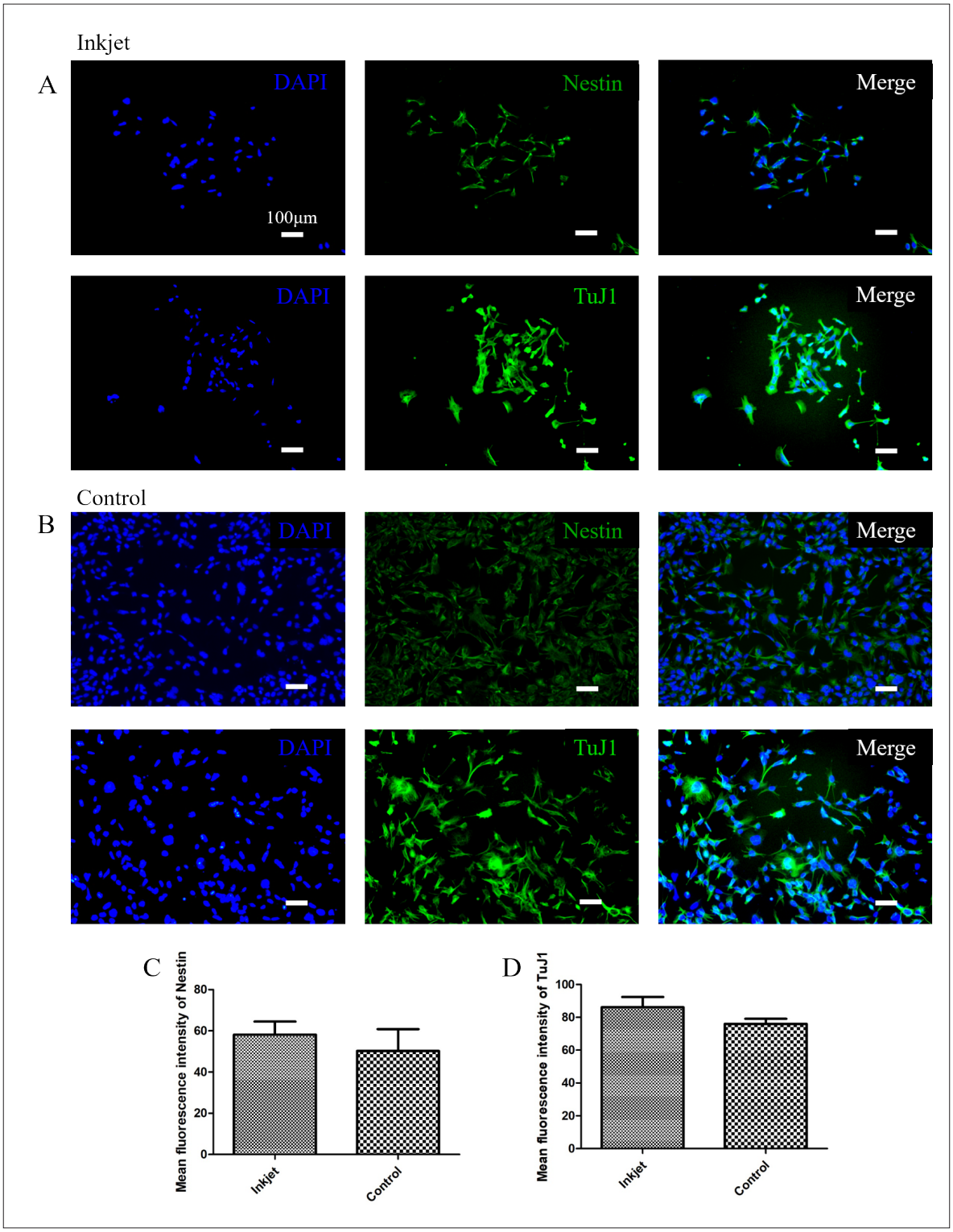


**Figure 6.** Nestin and TuJ1 immunofluorescence staining of inkjet-printed (inkjet) and manually pipetted (control) NE-4C cells at day five after retinoic acid treatment. (A) Fluorescent images of Nestin and TuJ1 for the inkjet group. Scale bar: 100 μm, magnification: 100×. (B) Fluorescent images of Nestin and TuJ1 for the control group. Scale bar: 100 μm, magnification: 100×. (C) Average fluorescence intensity of Nestin. (D) Average fluorescence intensity of TuJ1. Abbreviations: DAPI: 4',6-diamidino-2-phenylindole, TuJ1: Class III β-tubulin.

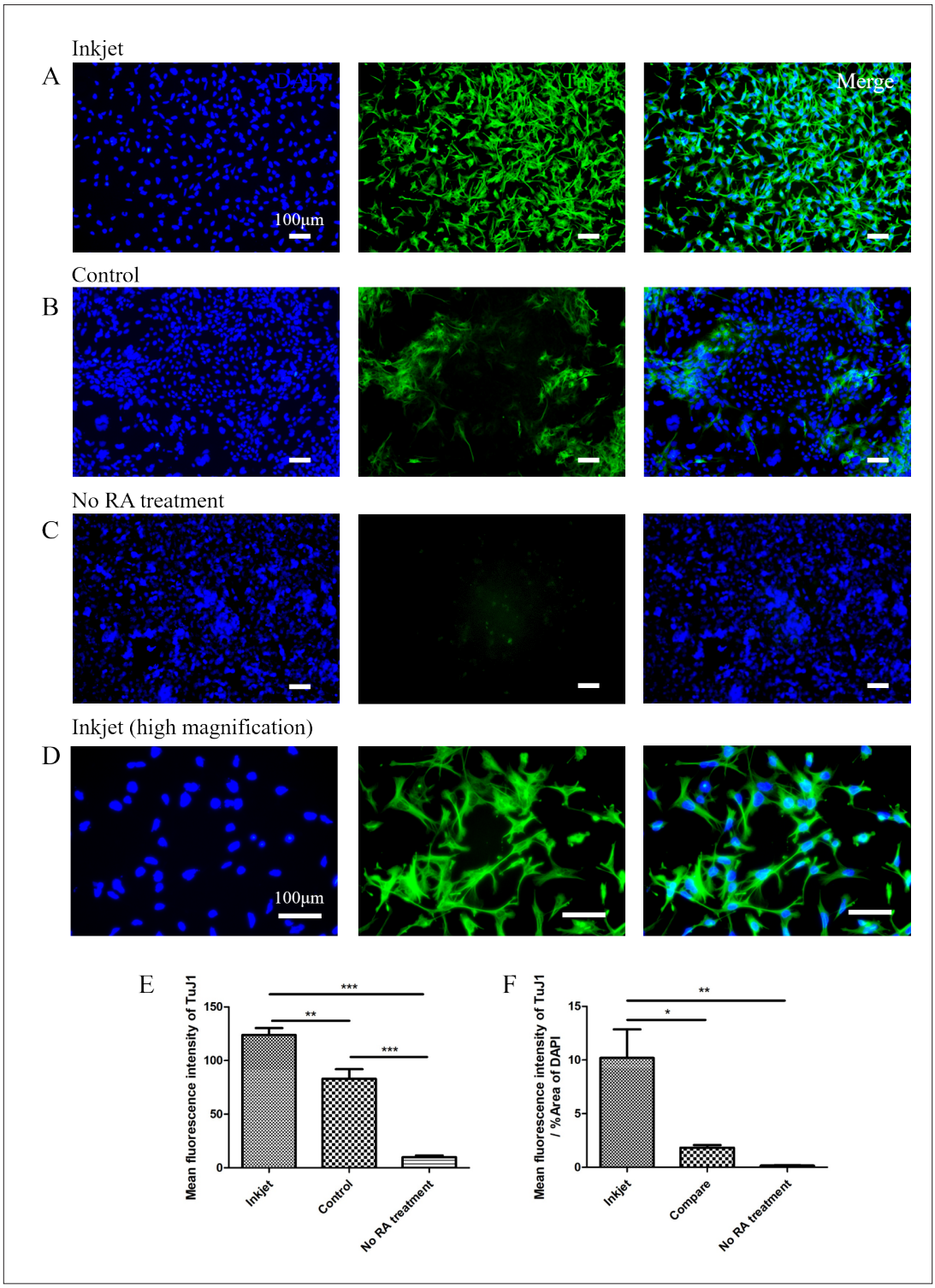


**Figure 7**. TuJ1 immunofluorescence staining of inkjet-printed (inkjet) and manually pipetted (control) NE-4C cells at day 8 after retinoic acid (RA) treatment. (A) Fluorescent images of TuJ1 for the inkjet and control groups. Scale bar: 100 μm, magnification: 100×. (B) Fluorescent images of TuJ1 for the control group. Scale bar: 100 μm, magnification: 100×. (C) Fluorescent images of TuJ1 for the no RA treatment group. Scale bar: 100 μm, magnification: 100×. (D) Fluorescent images of high magnification for the inkjet group. Scale bar: 100 μm, magnification: 200×. (E) Average fluorescence intensity of TuJ1. (F) The ratio of average fluorescence intensity and area of DAPI. Statistical significance determined at $^{*}p<0.05$, $^{**}p<0.01$, $^{***}p<0.001$. Abbreviation: DAPI: 4',6-diamidino-2-phenylindole, TuJ1: Class III β-tubulin.

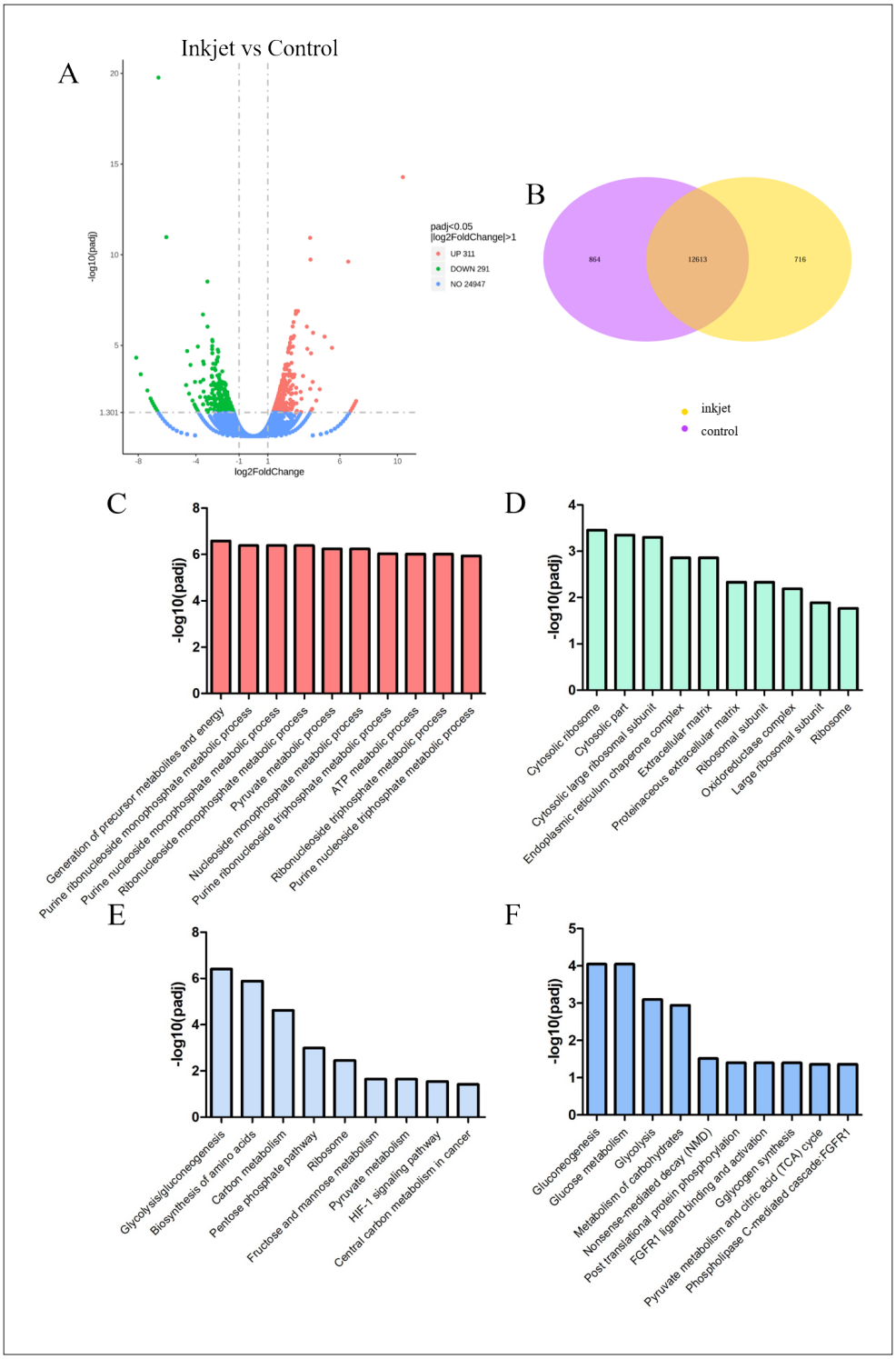


**Figure 8.** Results of RNA sequencing analysis of inkjet-printed (inkjet) and manually pipetted (control) on day 3 after printing. (A) The volcano plot of differential expression between the inkjet and control groups. (B) The Venn diagram. (C & D) Most significantly upregulated pathways for Gene Ontology enrichment analysis in terms of biological process and cellular component. (E) Most significantly upregulated pathways for Kyoto Encyclopedia of Genes and Genomes enrichment analysis. (F) Most significantly upregulated pathways for Reactome enrichment analysis. Abbreviation: padj: Adjusted *p*-value.

On day 8 after RA treatment, most of the cells in the inkjet group were TuJ1-positive, exhibiting further morphological changes compared to day 5 (Figure 7A & D). In contrast, a portion of cells in the control group were TuJ1-positive, with higher fluorescence intensity observed primarily in clustered cells (Figure 7B). Moreover, cells without RA treatment displayed minimal fluorescence intensity (Figure 7C). The average TuJ1 fluorescence intensities for the inkjet group, the control group, and the no RA treatment group were 123.82±14.52, 83.06±19.94, and 9.97±3.10, respectively (Figure 7E). Furthermore, the ratio of fluorescence intensity to the area of 4',6-diamidino-2-phenylindole staining was calculated to estimate differentiation efficiency. The values were 10.20±5.95 for the inkjet group, 1.84±0.51 for the control group, and 0.16±0.04 for the no RA treatment group (Figure 7F). Both measurements showed statistically significant differences between groups.

### 3.5. Difference in gene expression of NE-4C post-inkjet printing

After three days of culture, the inkjet-printed and manually pipetted (control) NE-4C cells were subjected to RNA-seq to assess differences in gene expression. As presented in Figure 8A, compared to the manually pipetted NE-4C cells, 311 genes were significantly upregulated and 291 genes downregulated in the inkjet group, indicating that inkjet bioprinting modulates gene expression in NE-4C cells. The Venn diagram further revealed 716 unique differential genes in the inkjet group, while 12,613 differential genes were common in both groups (Figure 8B). Gene Oncology (GO), Kyoto Encyclopedia of Genes and Genomes (KEGG), and Reactome enrichment analyses were performed to identify upregulated gene sets in inkjet-bioprinted NE-4C cells. In the GO biological process category, pathways related to cell metabolism were found to be significantly upregulated after inkjet bioprinting, including the generation of precursor metabolites and energy, pyruvate metabolic process, and adenosine triphosphate metabolic process (Figure 8C). In the GO cellular component category, ribosome-related pathways were significantly upregulated, including cytosolic ribosome, large ribosome subunit, and ribosome (Figure 8D). KEGG and Reactome analyses identified gluconeogenesis, biosynthesis of amino acids, and carbon metabolism-related pathways as being most significantly upregulated (Figure 8D & E). In summary, inkjet-bioprinted NE-4C cells exhibited an enhanced metabolic profile during the initial culture.

## 4. Discussion

In this study, NE-4C cells were directly printed into a culture dish containing culture medium using a thermal inkjet printhead. This method has previously been demonstrated to be feasible for creating cell patterns with high viability.[42] During inkjet bioprinting, the average number of cells in each ejected droplet depends on the nozzle diameter and cell concentration.[21,22] Here, a uniform NE-4C suspension with optimized cell concentration was used to increase the percentage of single-cell-containing droplets. This procedure ensured that most cells passed through the nozzle orifice under similar shear stress. Calcein-AM/PI staining was performed one hour post-bioprinting, at which point complete cell attachment had taken place. Under these conditions, 42.62% NE-4C were PI-positive, indicating the formation of transient pores on cell membranes that persisted for at least one hour. Considering that some pores likely resealed within this period, the actual percentage of cells with transient pores immediately after bioprinting may be higher than 42.62%.[43] Meanwhile, nearly all NE-4C were PI-negative and calcein-AM-positive one day after bioprinting, indicating that these transient pores were fully repaired. Given that the molecular weight of RA (300.44) is lower than that of PI (668.39), it is rational to hypothesize that RA would easily enter NE-4C through these transient pores.

During the initial four days after inkjet printing, a slower proliferation rate was found in inkjet-bioprinted NE-4C cells compared to manually pipetted cells, despite equal initial cell seeding densities. In a previous research, NG108-15 neuronal cells bioprinted using a 60 μm piezoelectric inkjet nozzle failed to exhibit significant proliferation slowdown during the initial incubation period.[32] In this study, a 30 μm nozzle was used, likely subjecting NE-4C cells to greater shear stress. A portion of NE-4C cells were found to be proliferating-inert while remaining attached to culture dishes and calcein-AM positive. Meanwhile, numerous cell clusters formed in the control group, whereas cells remained scattered in the inkjet group on day 4 post-bioprinting. Therefore, we infer that fewer proliferatively active NE-4C cells were present in the inkjet group, leading to a delayed proliferating peak.

Exposure to RA concentrations above $10^{-6}$M has been reported to be cytotoxic to carcinoma cells, and the recommended RA concentration for neural differentiation of NE-4C cells is $10^{-9}$–$10^{-6}$M.[37,38] In this study, we performed RA treatment immediately after inkjet printing and found that inkjet-bioprinted NE-4C cells exposed to $10^{-6}$ and $10^{-5}$M RA exhibited 1.91 times higher viability than manually pipetted NE-4C cells (Figure 4). It has been reported that NE-4C cells, upon reaching confluency, localize to the top of the basal layer.[36] According to the proliferating profile, it is clear that inkjet-bioprinted NE-4C would reach confluency later than the control group. Therefore, we consider that cells emerging from the basal

layer were more sensitive to RA and prone to detachment at higher RA concentrations ($10^{-5}$M). Moreover, at RA concentrations of $10^{-4}$M, the culture environment becomes excessively cytotoxic. Additionally, the inkjet group exhibited a higher percentage of TuJ1-positive cells at day 8 after a 48-hour RA treatment, indicating an enhanced tendency toward neuronal differentiation. Although RA treatment was performed immediately after inkjet printing, NE-4C cells undergo multiple mitotic cycles during the advanced stages of neural differentiation.[37] Neuronal fate decisions occur in randomly distributed, scattered cells governed by short-distance effects within local cell assemblies, which continue proliferating.[37] This phenomenon was observed in the control group, where randomly localized expressed TuJ1 at day 8 post-RA treatment. Since RA is needed to commit proliferating cells into neuronal progenitors, we believed the transient pores caused by inkjet bioprinting facilitated enhanced RA uptake during the initial treatment. Moreover, prolonged culture time (~4 weeks) is necessary for early neurons to mature and develop into neurons with various morphological patterns, during which antimitotic treatment should be applied.[37] Future studies are needed to provide stronger evidence evaluating the percentage of mature neurons produced by inkjet-bioprinted NE-4C cells.

NE-4C cells were collected on day 3 post-bioprinting for RNA-seq to evaluate gene expression differences between the inkjet and the control groups. GO, KEGG, and Reactome enrichment analyses revealed a higher level of cell metabolism in the inkjet group at this time point. In the biological process category, pathways related to nucleoside, pyruvate, and adenosine triphosphate metabolic processes were significantly upregulated. In the cellular component category, pathways related to ribosome biogenesis and components of the extracellular matrix were significantly upregulated. KEGG and Reactome analyses collectively suggested the upregulation of glucose and amino acid metabolic pathways. Taken together, these findings suggest that at day 3 post-bioprinting, a higher percentage of inkjet-printed NE-4C cells may be in the G1 or G2 phases of the cell cycle, during which the synthesis of amino acids and ribosomes is elevated to support cell growth and preparation for division. This deduction aligns with the observation that inkjet-printed NE-4C cells did not exhibit exponential proliferation during the initial 4-day culture period.

Shear stress during inkjet bioprinting is usually considered a detrimental effect. To mitigate cell damage, inkjet bioprinters often employ larger nozzle diameters (80–100 μm).[32,33] In this study, cell loss was observed due to the narrower nozzle used. However, previous research also found that shear stress is beneficial for gene transfection or specific cellular pathway activation.[27,34] We also found that NE-4C cells exhibited a stronger differentiation tendency under RA treatment following inkjet printing. This phenomenon might be partially attributed to transient pores induced in the cells during printing, facilitating RA molecule entry. However, additional pathway-related mechanisms likely contribute, warranting further investigation. Unlike hydrogel-encapsulated cell printing methods such as extrusion-based or laser-assisted printing, inkjet printing exerts direct influence on individual cells during droplet ejection. We believed that this nozzle-cell interaction represents a valuable avenue for further exploration.

## 5. Conclusion

In this study, NE-4C cells, a p53-deficient immortalized neuroectodermal progenitor cell line, were bioprinted for the first time using a 30 μm inkjet nozzle. Approximately 42.62% of cells exhibited transient pores an hour after printing. All transient pores were repaired within a day, and all attached cells remained viable. Following inkjet bioprinting, NE-4C cells demonstrated increased resistance to RA at concentrations ranging from $10^{-6}$ to $10^{-5}$M. Furthermore, inkjet-bioprinted NE-4C cells showed a higher level of TuJ1 expression on day 8 after RA treatment, indicating a stronger differentiation tendency. Additionally, RNA-seq analysis suggested that pathways related to cell metabolism were upregulated in inkjet-bioprinted NE-4C cells. Collectively, these results indicate that inkjet bioprinting could modulate NE-4C cell behavior and may represent a promising strategy for subcellular manipulation of neural progenitor cells.

## Acknowledgments

None.

## Funding

This research is supported by the National Natural Science Foundation of China (Grant No.52075285), the Applied Basic Research Project of Sichuan Province (Grant No.2021YJ0563), and the Natural Science Foundation of Sichuan Province (Grant No. 2023NSFSC0851).

## Conflict of interest

The authors declare they have no competing interests.

## Author contributions

*Conceptualization:* Xinda Li, Ruxiang Xu, Tao Xu
*Formal analysis:* Xinda Li, Huan Xiong
*Investigation:* Xinda Li, Xiaolei Guo

*Methodology:* Xinda Li, Jinzhou Feng, Lihua Chen
*Writing–original draft:* Xinda Li, Xiaolei Guo
*Writing–review & editing:* Xinda Li, Ruxiang Xu, Tao Xu

## Ethics approval and consent to participate

Not applicable.

## Consent for publication

Not applicable.

## Availability of data

Data will be made available upon request to the corresponding author.

## References


1. Saunders RE, Derby B. Inkjet printing biomaterials for tissue engineering: bioprinting. *Int Mater Rev*. 2014;59(8):430-448. doi: 10.1179/1743280414Y.0000000040.
2. Gudapati H, Dey M, Ozbolat I. A comprehensive review on droplet-based bioprinting: Past, present and future. *Biomaterials*. 2016;102:20-42. doi: 10.1016/j.biomaterials.2016.06.012.
3. Yeong WY, Chua C.K, Leong KF *et al*. Indirect fabrication of collagen scaffold based on inkjet printing technique. *Rapid Prototyping J*. 2006;12(4):229-237. doi: 10.1108/13552540610682741.
4. Zhang C, Wen X, Vyavahare NR, Boland T. Synthesis and characterization of biodegradable elastomeric polyurethane scaffolds fabricated by the inkjet technique. *Biomaterials*. 2008;29(28):3781-3791. doi: 10.1016/j.biomaterials.2008.06.009.
5. Inzana JA, Olvera D, Fuller SM, *et al*. 3D printing of composite calcium phosphate and collagen scaffolds for bone regeneration. *Biomaterials*. 2014;35(13): 4026-4034. doi: 10.1016/j.biomaterials.2014.01.064.
6. Campbell PG, Miller ED, Fisher GW, Walker LM, Weiss LE. Engineered spatial patterns of FGF-2 immobilized on fibrin direct cell organization. *Biomaterials*. 2005;26(33): 6762-6770. doi: 10.1016/j.biomaterials.2005.04.032.
7. Ilkhanizadeh S, Teixeira AI, Hermanson O, *et al*. Inkjet printing of macromolecules on hydrogels to steer neural stem cell differentiation. *Biomaterials*. 2007;28(27):3936-3943. doi: 10.1016/j.biomaterials.2007.05.018.
8. Miller ED, Li K, Kanade T Weiss LE, Walker LM, Campbell PG. Spatially directed guidance of stem cell population migration by immobilized patterns of growth factors. *Biomaterials*. 2011;32(11):2775-2785. doi: 10.1016/j.biomaterials.2010.12.005.
9. Xu T, Petridou S, Lee EH, *et al*. Construction of high-density bacterial colony arrays and patterns by the ink-jet method. *Biotechnol Bioeng*. 2004;85(1):29-33. doi: 10.1002/bit.10768.
10. Merrin J, Leibler S, Chuang JS. Printing multistrain bacterial patterns with a piezoelectric inkjet printer. *PLoS One*. 2007;2(7):e663. doi: 10.1371/journal.pone.0000663.
11. Yamazoe H, Tanabe T. Cell micropatterning on an albumin-based substrate using an inkjet printing technique. *J Biomed Mater Res A*. 2009;91(4):1202-1209. doi: 10.1002/jbm.a.32312.
12. Arai K, Iwanaga S, Toda H, Genci C, Nishiyama Y, Nakamura M. Three-dimensional inkjet biofabrication based on designed images. *Biofabrication*. 2011;3(3):034113. doi: 10.1088/1758-5082/3/3/034113.
13. Xu C, Chai W, Huang Y, Markwald RR. Scaffold-free inkjet printing of three-dimensional zigzag cellular tubes. *Biotechnol Bioeng*. 2012;109(12):3152-3160. doi: 10.1002/bit.24591.
14. Xu T, Zhao W, Zhu JM, Albanna MZ, Yoo JJ, Atala, A. Complex heterogeneous tissue constructs containing multiple cell types prepared by inkjet printing technology. *Biomaterials*. 2013;34(1):130-139. doi: 10.1016/j.biomaterials.2012.09.035.
15. Christensen K, Xu C, Chai W, Zhang Z, Fu J, Huang, Y. Freeform inkjet printing of cellular structures with bifurcations. *Biotechnol Bioeng*. 2015;112(5):1047-1055. doi: 10.1002/bit.25501.
16. Li X, Liu B, Pei B, *et al*. Inkjet Bioprinting of Biomaterials. *Chem Rev*. 2020 14;120(19):10793-10833. doi: 10.1021/acs.chem rev.0c00008.
17. Murphy SV, Atala A. 3D bioprinting of tissues and organs. *Nat Biotechnol*. 2014;32(8):773-785. doi: 10.1038/nbt.2958.
18. Xu T, Jin J, Gregory C, Hickman JJ, Boland T. Inkjet printing of viable mammalian cells. *Biomaterials*. 2005;26(1): 93-99. doi: 10.1016/j.biomaterials.2004.04.011.
19. Saunders RE, Gough JE, Derby B. Delivery of human fibroblast cells by piezoelectric drop-on-demand inkjet printing. *Biomaterials*. 2008;29(2):193-203. doi: 10.1016/j.biomaterials.2007.09.032.
20. Nakamura M, Kobayashi A, Takagi F, *et al*. Biocompatible inkjet printing technique for designed seeding of individual living cells. *Tissue Eng*. 2005;11(11-12):1658-1666. doi: 10.1089/ten.2005.11.1658.
21. Xu T, Kincaid H, Atala A, Yoo JJ. High-throughput production of single-cell microparticles using an inkjet printing technology. *J Manuf Sci E*. 2008;130(2):021017. doi: 10.1115/1.2903064.

22. Kim YK, Park JA, Yoon WH, Kim J, Jung, S. Drop-on-demand inkjet-based cell printing with 30-μm nozzle diameter for cell-level accuracy. *Biomicrofluidics*. 2016 30;10(6):064110. doi: 10.1063/1.4968845.

23. Stumpf F, Schoendube J, Gross A, *et al*. Single-cell PCR of genomic DNA enabled by automated single-cell printing for cell isolation. *Biosens Bioelectron*. 2015;69:301-306. doi: 10.1016/j.bios.2015.03.008.

24. Chen F, Lin L, Zhang J, He Z, Uchiyama K, Lin, J.M. Single-Cell Analysis Using Drop-on-Demand Inkjet Printing and Probe Electrospray Ionization Mass Spectrometry. *Anal Chem*. 2016;88(8):4354-4360. doi: 10.1021/acs.analchem.5b04749.

25. Dou R, Saunders RE, Mohamet L, Ward CM, Derby, B. High throughput cryopreservation of cells by rapid freezing of sub-μl drops using inkjet printing--cryoprinting. *Lab Chip*. 2015;15(17):3503-3513. doi: 10.1039/c5lc00674k.

26. Akiyama Y, Shinose M, Watanabe H, Yamada S, Kanda Y. Cryoprotectant-free cryopreservation of mammalian cells by superflash freezing. *Proc Natl Acad Sci USA*. 2019;116(16):7738-7743. doi: 10.1073/pnas.1808645116.

27. Xu T, Rohozinski J, Zhao W, Moorefield EC, Atala A, Yoo JJ. Inkjet-mediated gene transfection into living cells combined with targeted delivery. *Tissue Eng Part A*. 2009;15(1):95-101. doi: 10.1089/ten.tea.2008.0095.

28. Cui X, Dean D, Ruggeri ZM, Boland T. Cell damage evaluation of thermal inkjet printed Chinese hamster ovary cells. *Biotechnol Bioeng*. 2010;106(6):963-969. doi: 10.1002/bit.22762.

29. Sohrabi S, Liu Y. Modeling thermal inkjet and cell printing process using modified pseudopotential and thermal lattice Boltzmann methods. *Phys Rev E*. 2018;97(3-1):033105. doi: 10.1103/PhysRevE.97.033105.

30. Das SR, Uz M, Ding S, *et al*. Electrical differentiation of mesenchymal stem cells into Schwann-Cell-Like phenotypes using inkjet-printed graphene circuits. *Adv Healthc Mater*. 2017;6(7):1601087. doi: 10.1002/adhm.201601087.

31. Zips S, Huang B, Hotte S, *et al*. Aerosol Jet-Printed High-Aspect ratio Micro-Needle electrode arrays applied for human cerebral organoids and 3D neurospheroid networks. *ACS Appl Mater Interfaces*. 2023;15(30):35950-35961. doi: 10.1021/acsami.3c06210.

32. Tse C, Whiteley R, Yu T, *et al*. Inkjet printing Schwann cells and neuronal analogue NG108-15 cells. *Biofabrication*. 2016;8(1):015017. doi: 10.1088/1758-5090/8/1/015017.

33. Lorber B, Hsiao WK, Hutchings, IM, Martin KR. Adult rat retinal ganglion cells and glia can be printed by piezoelectric inkjet printing. *Biofabrication*. 2014;6(1):015001. doi: 10.1088/1758-5082/6/1/015001.

34. Solis LH, Ayala Y, Portillo S, Varela-Ramirez A, Aguilera R, Boland, T. Thermal inkjet bioprinting triggers the activation of the VEGF pathway in human microvascular endothelial cells in vitro. *Biofabrication*. 2019;11(4):045005. doi: 10.1088/1758-5090/ab25f9.

35. Yumoto M, Hemmi N, Sato N, *et al*. Evaluation of the effects of cell-dispensing using an inkjet-based bioprinter on cell integrity by RNA-seq analysis. *Sci Rep*. 2020;10(1):7158. doi: 10.1038/s41598-020-64193-z.

36. Schlett K, Herberth B, Madarász E. In vitro pattern formation during neurogenesis in neuroectodermal progenitor cells immortalized by p53-deficiency. *Int J Dev Neurosci*. 1997;15(6):795-804. doi: 10.1016/s0736-5748(97)00015-4.

37. Schlett K, Madarász E. Retinoic acid induced neural differentiation in a neuroectodermal cell line immortalized by p53 deficiency. *J Neurosci Res*. 1997;47(4):405-415.

38. Strickland S, Mahdavi V. The induction of differentiation in teratocarcinoma stem cells by retinoic acid. *Cell*. 1978;15(2):393-403. doi: 10.1016/0092-8674(78)90008-9.

39. Maden, M. Retinoic acid in the development, regeneration and maintenance of the nervous system. *Nat Rev Neurosci*. 2007;8(10):755-765. doi: 10.1038/nrn2212.

40. Napoli JL. Interactions of retinoid binding proteins and enzymes in retinoid metabolism. *Biochim Biophys Acta*. 1999;1440(2-3):139-162. doi: 10.1016/s1388-1981(99)00117-1.

41. Ables JL, Decarolis NA, Johnson MA, *et al*. Notch1 is required for maintenance of the reservoir of adult hippocampal stem cells. *J Neurosci*. 2010;30(31):10484-10492. doi: 10.1523/JNEUROSCI.4721-09.2010.

43. Park JA, Yoon S, Kwon J, *et al*. Freeform micropatterning of living cells into cell culture medium using direct inkjet printing. *Sci Rep*. 2017;7(1):14610. doi: 10.1038/s41598-017-14726-w.

43. Barui S, Saunders RE, Naskar S, Basu B, Derby B. Acoustic poration and dynamic healing of mammalian cell membranes during inkjet printing. *ACS Biomater Sci Eng*. 2020;6(1):749-757. doi: 10.1021/acsbiomaterials.9b01635.